Adsorption 11: 455–460, 2005
© 2005 Springer Science + Business Media, Inc. *Manufactured in The Netherlands.*

Internal Transport Resistances and their Influence on Diffusion in Zeolites as Traced by Microscopic Measuring Techniques

CHRISTIAN CHMELIK, PAVEL KORTUNOV, SERGEY VASENKOV AND JÖRG KÄRGER*
Universität Leipzig, Institut für Physik, Abt. GFP, Linnéstraße 5, D-04103 Leipzig, Germany
kaerger@physik.uni-leipzig.de

Abstract. Interference microscopy (IFM) and FTIR microscopy (IRM) are applied to study intracrystalline concentration profiles in SAPO-5, CrAPO-5 and ZSM-5 zeolite crystals. By using both techniques, the high spatial resolution of interference microscopy is complemented by the ability of FTIR spectroscopy to pinpoint adsorbates by their characteristic IR bands. In this way the experimental results are shown to unveil a number of remarkable deviations in the real structure of zeolite crystals from their textbook patterns. The influence of structural defects on the equilibrium concentration profiles as well as on sorption dynamics of guest molecules is investigated. Owing to the ability to gain direct insight into the influence of surface defects and intracrystalline defects on molecular uptake, the applied techniques give more accurate information on the molecular transport in zeolite crystals than the classical uptake methods.

Keywords: zeolite, diffusion, concentration profiles, defects, interference microscopy

1. Introduction

Among different types of nanoporous materials zeolites are famous for their well-defined morphology (Baerlocher et al., 2001). Due to their unique properties zeolites are broadly used as catalysts and molecular sieves in different fields of applied chemistry and technology. In many of these applications molecular transport is of crucial importance. For theoretical understanding of transport processes, which is needed for further optimization and application of new concepts, it is essential to know how the molecular transport is influenced by various features of zeolite structure (such as pore system, intergrowth effects and transport barriers and defects on the external crystal surface).

Intracrystalline transport in zeolites has been a subject of a large number of recent theoretical and experimental studies (Auerbach, 2000; Chen et al. 1994; Kärger et al., 1992, 2003; Theodorou et al., 1996). While the ideal structure of zeolites is routinely used to elucidate their adsorption and transport properties it was only recently appreciated that these properties can be influenced to a great extent by building defects of the crystals (Kärger et al., 2002, 2003). Direct studies of the role of crystal surface and structure in molecular uptake has become available only recently with the introduction of the interference microscopy technique in our laboratory. This technique is capable of monitoring intracrystalline concentration profiles for a selected zeolite crystal during molecular adsorption or desorption with an unprecedented spatial resolution, as it will be shown in the present work.

Such investigations are also important in view of the persistent differences between intracrystalline diffusivities obtained for the same zeolites by different experimental techniques (Auerbach, 2000; Chen et al., 1994; Kärger et al., 1992, 2002, 2003; Theodorou et al., 1996). The discrepancies are especially large between the diffusivities measured by the microscopic techniques, i.e. by such techniques as pulsed field gradient (PFG) NMR and quasi-elastic neutron scattering (QENS), which are capable of probing much smaller molecular displacements than the size of individual crystals, and by the classical uptake techniques, which

*To whom correspondence should be addressed.

measure overall adsorption/desorption. Since the influence of the defects may strongly depend on the probed length scale and on the type of experiment, explanations for the differences may be found. For example, the apparent diffusivities determined by uptake methods will obviously be reduced if surface resistance to mass transfer is significant. This resistance, however, will not influence the PFG NMR results for molecular displacements smaller than the crystal size.

2. Methods and Materials

The interference and IR microscopy techniques are the only two techniques, which are proved to be suitable for monitoring of intracrystalline concentration profiles of guest molecules in zeolite crystals. The detailed description of these techniques may be found in Geier et al. (2001a, b); Lehmann et al. (2002), and Schemmert et al. (1999a, b). Briefly, the interference microscopy method is based on the changes of the optical density of porous crystals following adsorption or desorption of guest molecules. Expecting proportionality of the refractive index and the local concentration of guest molecules in the crystal, the experimental data allow to determine a value proportional to the integral of the local concentration in the direction of light propagation. The concentration integrals are recorded with the spatial resolution of $\sim 0.5 \times 0.5\ \mu m^2$.

The concentration integrals were also monitored in a somewhat more direct way by using the IR microscopy method (IRM) for recording the IR absorbance spectra of guest molecules residing in a crystal. Despite a poor spatial resolution, IR microscopy presents an extremely useful tool to study intracrystalline concentration profiles due to its ability to distinguish between different adsorbates. Thus, it opens the possibility for tracer-exchange, counter- and co-diffusion measurements (Hermann et al., 1995; Karge et al., 1996; Niessen et al., 1993).

The measurement set-up consists of a vacuum system and a JENAPOL interference microscope (Carl Zeiss GmbH) with an interferometer of Mach-Zehnder type for interference microscopy measurements, and of the IR microscope UMA 500 attached to the FTIR spectrometer FTS 6000 (Digilab), which is equipped with a motorized stage, for IR microscopy measurements. Interference patterns were recorded during adsorption and desorption by a CCD camera (XC-77CE, Sony).

SAPO-5 and CrAPO-5 belong to the AFI-type molecular sieves (Baerlocher et al., 2001). The samples of SAPO-5 and CrAPO-5 were prepared and calcined as described in Kornatowski et al. (2001), Padlyak et al. (2000), Schüth et al. (1994); Schunk et al. (1996). The chromium content of CrAPO-5 was 0.25 Cr per u.c.. Methanol and water were used as guest molecules for CrAPO-5 and SAPO-5.

Two calcined samples of zeolite ZSM-5 with a Si/Al ratio around 40 and a mean crystal size of $50 \times 50 \times 140\ \mu m^3$ were used for the measurements. The samples were prepared from the same as-synthesized zeolite ZSM-5 following two different procedures (Wloch, 2003): while the first sample (i.e. the non-etched sample) is the calcined as-synthesized zeolite, the second sample (i.e. the etched sample) was first subjected to the etching in an aqueous solution of HF with acetone, and only then calcined. Following the procedure suggested by Wloch the etching was carried out to remove the outer layers, which may contain various defects and impurities, from the zeolite crystal surface. Isobutane (Aldrich, 99%) was used as an adsorbate.

For the measurements and activation the zeolite sample was introduced into a specially made optical or IR cell connected to the vacuum system. Prior to the measurements, the sample was activated by keeping it under high vacuum at elevated temperature (typically at around 200°C) for over 12 h. The measurements of the concentration integrals were always performed at room temperature with one selected zeolite crystal. The adsorption or desorption has been initiated by appropriate changes of adsorbate pressure in the surrounding gas phase. The measurements of the concentration profiles in all cases were carried out with at least 6 different crystals to make sure that the results are reproducible.

3. Results and Discussion

The ideal framework topology of AFI-type zeolites can be described as a hexagonal packing of identical oriented cylinders (Baerlocher et al., 2001). This textbook structure can hardly be found compatible with the equilibrium intracrystalline concentration profiles of methanol in CrAPO-5 crystals (Fig. 1(a)). The profiles in Fig. 1(a) were recorded using the interference microscopy (IFM) technique under equilibrium with the methanol vapour in the gas phase surrounding the crystal (Lehmann et al., 2002). The highly inhomogeneous profiles in Fig. 1(a) exhibit the reproducible regular patterns characteristic for regular intergrowth effects. An existence of the intergrowth structure was confirmed by an observation of unloaded crystals

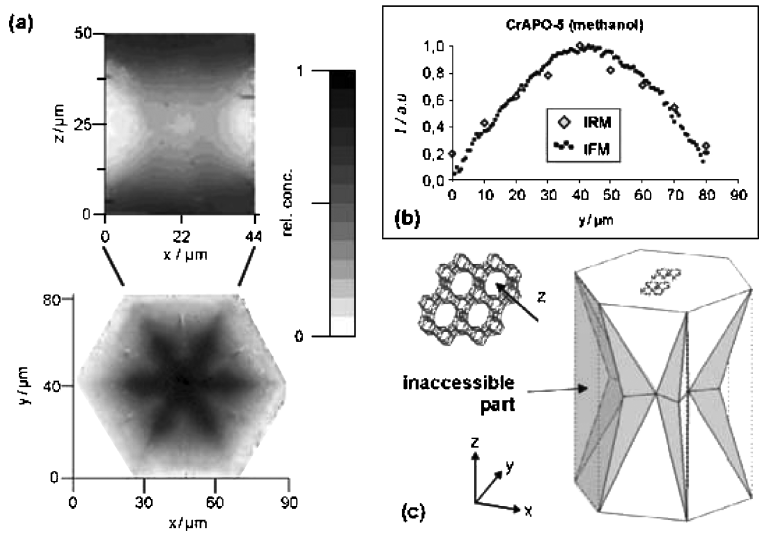

Figure 1. (a) IFM equilibrium intracrystalline concentration profile of methanol in a CrAPO-5 crystal. The color intensity is proportional to the integrals of local concentration. (b) Comparison of mean concentration integrals I recorded by IRM and IFM. (c) Suggested internal structure. The channel direction coincides with the z direction.

under crossed Nicols. This structure renders a part of the channels to be inaccessible for methanol molecules. Based on the recorded profiles the internal structure of the CrAPO-5 crystals was proposed. This structure is shown in Fig. 1(c) (Lehmann et al., 2003). The semi-pyramids in Fig. 1(c) outline schematically the crystal sections accessible for methanol. The channel direction in the semi-pyramids coincides with the z direction.

To confirm the results obtained by interference microscopy, the equilibrium intracrystalline concentration profiles of methanol in CrAPO-5 crystals were recorded under the same measurement conditions by IR microscopy (Lehmann et al., 2002). Due to much lower spatial resolution of IR microscopy ($20 \times 20\ \mu m^2$) a direct comparison of two-dimensional concentration profiles obtained by these two techniques is not feasible. Instead, the one-dimensional profiles along the y and z directions have been compared. Figure 1(b) demonstrates good agreement between the results obtained by both techniques.

The results discussed above clearly show that the investigated crystals cannot by far be considered as ideal AFI crystals. Intergrowth effects similar to those shown in Fig. 1(c) were frequently observed in other AFI-type crystals synthesized in solution (Girnus et al., 1994; Klap et al., 1999, 2000). For some of these crystals it was shown that only the internal crystal components, which resemble geometrically the semi-pyramids in Fig. 1(c), could be loaded with adsorbate (Girnus et al., 1994).

Concentration profiles of methanol during its adsorption into the one-dimensional channels of CrAPO-5 crystals are reported in Lehmann et al. (2003a). They have shown the existence of a surface resistance, which hinders the uptake significantly. By comparing the IFM results with dynamic Monte Carlo simulations the influence of the internal structure and surface barriers on intracrystalline diffusion of methanol was investigated quantitatively (Lehmann et al., 2003a).

Figure 2 shows the intracrystalline concentration profiles of water in CrAPO-5 and SAPO-5 measured by IFM (Lehmann et al., 2003b). It is seen that the profiles obtained for low pressure of 1 mbar reveal highly inhomogeneous, but reproducible patterns. It is noteworthy that the profiles in CrAPO-5 (Fig. 2 (a1) and (a3)) resemble, to some extent, the methanol profiles observed for these crystals (Fig. 1(a)). Apparently, the existence of the intergrowth structure (Fig. 1(c)) is also responsible for the inhomogeneous intracrystalline distribution of water molecules in these crystals. Different concentration of Cr atoms and/or of defect site in the different crystal components may result in the observed nonhomogeneous profiles. The origin of the intergrowth effects may be derived from the progress of the crystal growth. As has been shown in (Schunk et al., 1996)

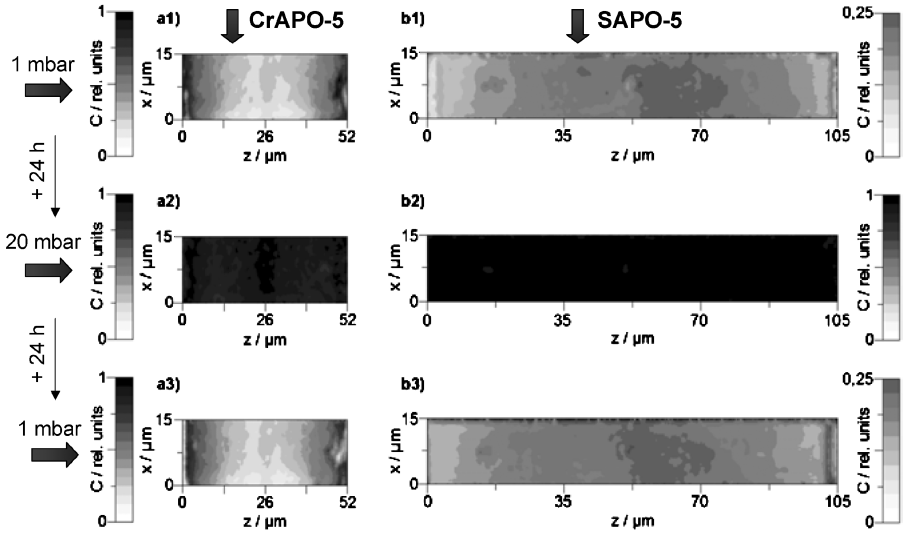

Figure 2. Intracrystalline concentration profiles of water in the CrAPO-5 (a1, a2, a3) and SAPO-5 (b1, b2, b3) crystals integrated along the y direction under equilibrium with water vapor at 1 mbar (a1, b1, a3, b3) and 20 mbar (a2, b2). The profiles under the pressure of 1 mbar were recorded after change of the water pressure form 0 to 1 mbar (a1, b1) and from 20 to 1 mbar (a3, b3). The channels run along the z axis. Darker regions correspond to higher concentration integrals.

the dumbbell shape is characteristic for some AFI-type crystals in the intermediate stage of growth.

The inhomogeneous profiles of water in SAPO-5 Fig. 2(b1) and (b3) may result from a structural heterogeneity of the crystals as well. Indeed, it has been shown by electron microprobe analysis that the silicon content in the central part of the SAPO-5 crystals is lower by a factor of 2 to 3 than at the crystal margins (Schunk et al., 1996).

The increase in water vapor pressure to 20 mbar results in an essentially homogeneous profiles in both samples (Fig. 2(a2) and (b2), i.e. the whole crystal is equally filled with liquid-like water. In this case the level of the water loading is no longer influenced by the water interaction with the zeolite framework. Instead, it is determined by the available zeolite pore volume.

All profiles were recorded 6 h after applying the pressure step. During the following 18 h, no changes in the profiles were observed, which suggests that the profiles in Fig. 1 reflect the intracrystalline water distribution under equilibrium with the gas phase. The equilibrium nature of the profiles at the water pressure of 1 mbar was confirmed by the fact that essentially identical profiles were obtained following the change of the water vapor pressure from 0 to 1 mbar and from 20 to 1 mbar (Fig. 2).

Figures 3(a) and (b) show the images of a typical ZSM-5 crystal for the two different crystal orientations. In addition to the typical hourglass structure (Agger et al., 2003; Hay et al., 1990; Geus et al., 1994; Weidenthaler et al., 1994), the majority of the crystals reveal line-like defects (see the crystal image in Fig. 3(a), which run along the z-direction through the central part of the crystals. It is important to note that in each particular crystal such defect was usually detected only on a single (i.e. either on the (z, x) or on the (z, y)) crystal face.

Figures 3(c)–(f) show the evolution of the intracrystalline concentration profiles during isobutane desorption. While the c- and d-sections of the figures present 2-dimensional concentration profiles, the sections e and f show profiles along the x- or y-direction in the central part of the crystals. The profiles in sections c and e reveal anomalous desorption patterns: in the middle part of the crystals the desorption proceeds faster than near the crystal edges. Noting that the areas of fastest desorption are located around the line-like defects, one may conclude that these defects represent cracks opening an additional route for isobutane adsorption/desorption. This additional route causes the non-symmetric shape of the profiles in Fig. 3(d) and (f).

The overall shape of the concentration profiles obtained for the crystals from the non-etched sample

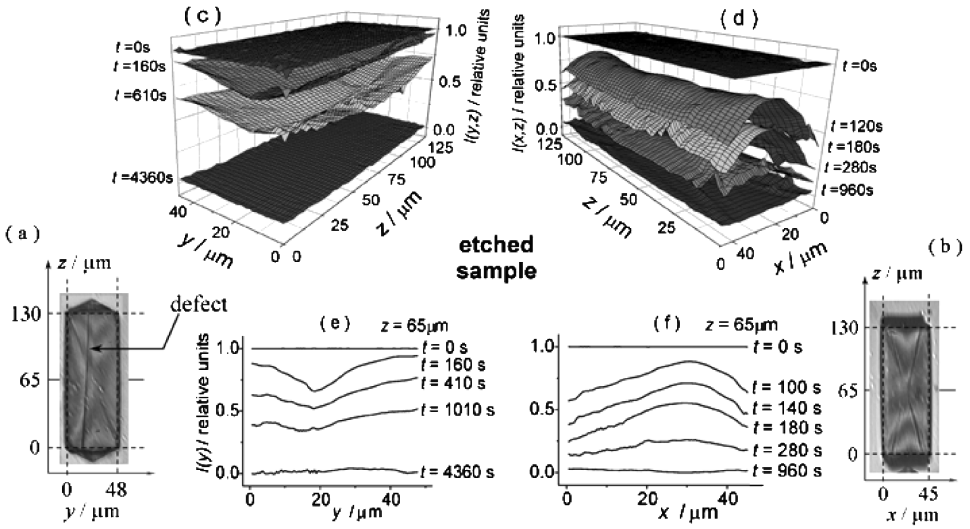

Figure 3. Microscopic images of the crystal and intracrystalline concentration profiles of isobutane recorded by IFM during the desorption of isobutane in etched ZSM-5 crystals. The observation direction was perpendicular to the (z, y) plane in a, c, e and perpendicular to the (z, x) plane in b, d, f. The desorption was initiated by a rapid change of the isobutane pressure in the cell from 10 to 0 mbar. The concentration integrals $I = 1.0$ correspond to those measured under equilibrium with an isobutane pressure of 10 mbar. The t values shown in c, d, e, f indicate the time intervals after the start of desorption.

(Kortunov et al., 2004) is in a striking contrast with the shape, which can be expected for desorption through the outer surface of the crystal assuming that the intracrystalline diffusion is the rate-determining process (Geier et al., 2001a, b). Indeed, we have not observed any pronounced concentration decrease near the crystal edges in the transient concentration profiles, which are to be expected in the latter case. This result suggests the existence of strong transport barriers on the crystal surface (excluding the surface of the cracks), which mainly determine the rate of adsorption/desorption. The existence of transport barriers on the external surface of ZSM-5 crystals have already been reported in a number of papers (Kärger et al., 1991; Micke et al., 1994; Wloch, 2003). As demonstrated by Figs. 3(d) and (f) the acid treatment of the crystals has decreased the strength of such surface barriers significantly. As a result, the concentration profiles look more similar to the ones, which are expected for a diffusion-controlled process.

Comparison of the shape of the measured profiles with that obtained by dynamic Monte Carlo (MC) simulations has allowed us to rule out, for the studied crystals, the possibility of a rapid uptake of isobutane through the internal intersections directly from the gas phase surrounding the crystals (Geier et al., 2001a, b).

4. Summary

Monitoring intracrystalline concentration profiles opens a new, direct way to study the influence of intracrystalline defects and of defects on external crystal surface on molecular uptake. In the present work we have presented several examples of the analysis of concentration profiles of guest molecules, which allows to get information on such influence. In particular, it was shown that defects on the external crystal surface are able to increase or to decrease the rate of adsorption/desorption. The former is associated with the existence of an additional adsorption/ desorption pathway, namely with the adsorption/desorption through cracks in the crystal surface, as shown for the MFI samples. The latter has its origin in the blockage or structural changes of the external crystal surface leading to the appearance of surface barriers (CrAPO-5 and ZSM-5). In addition, the influence of intergrowth effects on uptake was discussed (CrAPO-5).

Acknowledgment

The zeolite samples have been synthesized in the groups of J. Kornatowski, F. Schüth and by J. Wloch. We thank these colleagues for supplying us with these

samples, as well as D.M. Ruthven and J. Weitkamp for numerous stimulating discussions. Financial support by Deutsche Forschungsgemeinschaft (International Research Group "Diffusion in Zeolites" and International Research Training Group 1056 "Diffusion in Porous Materials"), Fonds der Chemischen Industrie and Max-Buchner-Forschungsstiftung is gratefully acknowledged.

References

Agger, R.A., N. Hanif, C.S. Cundy, A.P. Wade, S. Dennison, P.A. Rawlinson, and M.W. Anderson, *J. Am. Chem. Soc.*, **125**, 830 (2003).

Auerbach, S.M., *Int. Rev. Phys. Chem.,* **19**, 155 (2000).

Baerlocher, Ch., W.M. Meier, and D.H. Olson, *Atlas of Zeolite Framework Types*, Elsevier, Amsterdam, 2001, pp. 34–35.

Chen, N.Y., T.F. Degnan, and C.M. Smith, *Molecular Transport and Reaction in Zeolites,* VCH, New York, 1994.

Geier, O., S. Vasenkov, E. Lehmann, J. Kärger, U. Schemmert, R.A. Rakoczy, and J. Weitkamp, *J. Phys. Chem. B*, **105**, 10217–10222 (2001a).

Geier, O., S. Vasenkov, E. Lehmann, J. Kärger, U. Schemmert, R.A. Rakoczy, and J. Weitkamp, *Stud. Surf. Sci. Catal.*, **135**, 154–160 (2001b).

Geus, E.R., J.C. Jansen and H. van Bekkum, *Zeolites*, **14**, 82 (1994).

Girnus, L., K. Jancke, R. Vetter, J. Richter-Mendau and J. Caro, *Zeolites*, **15**, 33 (1995).

Hay, D.G., H. Jaeger, and K.G. Wilshier, *Zeolites*, **10**, 571 (1990).

Hermann, M., W. Niessen, and H.G. Karge, *Stud. Surf. Sci. Catal.*, **94**, 131–138 (1995).

Karge, H.G., W. Niessen, and H. Bludau, *Applied Catalysis A:* General, **146**, 339–349 (1996).

Kärger, J. and H. Pfeifer, *J. Chem. Soc. Faraday Trans.*, **87**, 1989 (1991).

Kärger, J. and D.M. Ruthven, *Diffusion in Zeolites and Other Microporous Solids,* Wiley & Sons, New York, 1992.

Kärger, J. and D.M. Ruthven, "Diffusion and Adsorption in Porous Solids," in *Handbook of Porous Solids*, F. Schüth, K.S.W. Sing, and J. Weitkamp (Eds.), p. 2089, Wiley-VCH, Weinheim, 2002.

Kärger, J., S. Vasenkov, and S.M. Auerbach, "Diffusion in Zeolites," in *Handbook of Zeolite Science and Technology*, S.M. Auerbach, K.A. Carrado, and P.K. Dutta, (Eds.), p. 341, Marcel-Dekker Inc., New York, 2003.

Klap, G.L., H. van Konnigsveld, H. Graafsma, and A.M.M. Schreurs, *Microporous and Mesoporous Materials*, **38**, 403 (2000).

Klap, G.L., M. Wübbenhorst, J.C. Jansen, H. van Konnigsveld, H. van Bekkum, and J. van Turnhout, *Chem. Mater.*, **11**, 3497–3503 (1999).

Kornatowski, J., G. Zadrozna, M. Rozwadowski, B. Zibrowius, F. Marlow, and J.A. Lercher, *Chem. Mater.*, **13**, 4447–4456 (2001).

Kortunov, P., S. Vasenkov, C. Chmelik, J. Kärger, D.M. Ruthven, and J. Wloch, *Chem. Mater.*, **16**, 3552–3558 (2004).

Lehmann, E., C. Chmelik, H. Scheidt, S. Vasenkov, B. Staudte, J. Kärger, F. Kremer, G. Zadrozna, and J. Kornatowski, *J. Am. Chem. Soc.* **124**, 8690–8692 (2002).

Lehmann, E., S. Vasenkov, J. Kärger, G. Zadrozna, and J. Kornatowski, *J. Chem. Phys.*, **118**, 6129 (2003a).

Lehmann, E., S. Vasenkov, J. Kärger, G. Zadrozna, J. Kornatowski, Ö. Weiss, and F. Schüth, *J. Phys. Chem. B*, **107**, 4685–4687 (2003b).

Micke, A., M. Bulow, and M. Kocirik, *J. Phys. Chem.*, **98**, 924 (1994).

Niessen, W. and H.G. Karge, *Microporous Materials*, **1**, 1–8 (1993).

Padlyak, B.V., J. Kornatowski, G. Zadrozna, M. Rozwadowski, and A. Gutsze, *J. Phys. Chem. A*, **51**, 11837–11843 (2000).

Schemmert, U., J. Kärger, C. Krause, R.A. Rakoczy, and J. Weitkamp, *Europhys. Lett.*, **46**, 204 (1999a).

Schemmert, U., Kärger, J. and J. Weitkamp, *Microporous and Mesoporous Materials*, **32**, 101 (1999b).

Schunk, S.A., D.G. Demuth, B. Schulz-Dobrick, K.K. Unger, and F. Schüth, *Microporous Mater.*, **6**, 273–285 (1996).

Schüth, F., D.G. Demuth, B. Zibrowius, J. Kornatowski, and G. Finger, *J. Am. Chem. Soc*., **116**, 1090 (1994).

Theodorou, D.N., R.Q. Snurr, and A.T. Bell, "Molecular Dynamics and Diffusion in Microporous Materials," in *Comprehensive Supramolecular Chemistry*, G. Alberti, and T. Bein, (Eds.), p. 507, Pergamon Press, Oxford, 1996.

Weidenthaler, C., R.X. Fischer, R.D. Shannon, and O. Medenbach, *J. Phys. Chem.*, **98**, 12687 (1994).

Wloch, J., *Microporous Mesoporous Mater.*, **62**, 81 (2003).